

19th CIRP Conference on Electro Physical and Chemical Machining, 23-27 April 2018, Bilbao, Spain

## Ablation Investigation of Cemented Carbides Using Short-Pulse Laser Beams

Shiqi Fang<sup>a,b,c</sup>, Rita Lima<sup>a,b</sup>, Daniela Sandoval<sup>a,b</sup>, Dirk Bähre<sup>c</sup> and Luis Llanes<sup>a,b,\*</sup>

<sup>a</sup>*CIEFMA – Dept. Materials Science and Engineering, Universitat Politècnica de Catalunya, EEBE-Campus Diagonal Besòs, Barcelona, 08019, Spain*

<sup>b</sup>*Barcelona Research Center in Multiscale Science and Engineering, Universitat Politècnica de Catalunya, Barcelona, 08019, Spain*

<sup>c</sup>*Institute of Production Engineering, Saarland University, Saarbrücken, 66123, Germany*

\* Corresponding author. Tel.: +34 (0) 93 401 10 83; fax: +34 (0) 93 401 67 06. E-mail address: [luis.miguel.llanes@upc.edu](mailto:luis.miguel.llanes@upc.edu)

### Abstract

As an excellent engineering tool material, cemented carbides are capable to shape and cut metallic materials with high surface finish quality and precision. However, in regard to conventional abrasive methods cemented carbides are difficult-to-machine materials due to their extreme hardness combined with relatively low toughness. In contrast, laser beam machining is an advanced non-contacting cutting method which is therefore suitable for shaping hard materials. In particular, the application of short-pulse laser beams enables the cutting of hard materials meeting high precision requirements. Moreover, it can effectively reduce defects induced by mechanical contacts and thermal reactions. In this paper, a general study of the ablation mechanism of cemented carbides using short-pulse laser is conducted. Special attention is paid to the correlation between the material ablation and machining parameters within the nanosecond regime: pulse number and pulse energy. In doing so, two cemented carbide grades with similar composition but different grain size have been chosen as investigated materials. An experimental set-up equipped with a nanosecond laser and an auto-stage is implemented to produce dimples on the cemented carbide surfaces with variable pulse number and pulse energy. The experimental design and characterization of geometrical features of produced dimples are presented and discussed. The work is complemented with a thorough surface integrity assessment of the shaped materials. It is found that ablation increases proportionally with the pulse number and applied energy. Regarding microstructural effects, ablation is discerned to be more pronounced in the coarse-grained grade as compared to the medium-sized one.

© 2018 The Authors. Published by Elsevier B.V. This is an open access article under the CC BY-NC-ND license (<http://creativecommons.org/licenses/by-nc-nd/4.0/>).

Peer-review under responsibility of the scientific committee of the 19th CIRP Conference on Electro Physical and Chemical Machining

*Keywords:* cemented carbides; laser beam machining; short-pulse laser; surface integrity.

### 1. Introduction

WC-Co cemented carbides are composite materials widely used in demanding applications such as cutting and wear-resistant parts, due to their remarkable combination of hardness and toughness. Such exceptional properties result from the successful sintering of tungsten carbides (WC) as the hard phase and cobalt (Co) as the tough binder one under high temperature and pressure [1-3]. WC merges physical properties of ceramics and electronic properties of metals. This yields particles with high hardness and good thermal and electrical conductivities [4]. Mechanical properties of cemented carbides strongly rely on their microstructure and composition [1-2]. For instance, cemented carbides with medium grain size (~1 μm)

are used as wear-resistant mechanical parts or cutting tools when shock endurance and abrasion resistance are required. Meanwhile, grades with coarse grain size (> 2.5 μm) are used in oil, gas and mining applications when a high impact strength is needed [1-2, 5-6]. In general, the hardness increases when grain size and binder content decrease, resulting in a loss of toughness as a collateral effect [2].

Laser beam machining is an advanced processing technique in the industry. It is capable to shape hard engineering materials, especially cemented carbides, which are difficult to machine using conventional cutting methods, such as milling and grinding [7, 8]. Laser beam machining can deliver high power density to a limited area on the targeted material surface, which results in precise and efficient material ablation [9-12].

Due to its high coherence, monochromaticity and energy density, laser beam ablation is a powerful tool in machining hard (and brittle) materials. These properties point out laser machining as suitable for almost any advanced engineering materials [11-13].

Laser beam machining shows some important advantages, especially when it involves short or ultra-short pulse laser beams. For example, surface damage can be effectively avoided using this contact-free and precise processing [7, 11-12, 14]. In the short-pulse regime, i.e. nanosecond, materials are mainly ablated by melting and subsequent vaporization [9-10, 12, 15]. For WC-Co cemented carbides, the difference of melting and vaporization temperatures between WC and Co results in two different laser-matter behaviors. WC's melting temperature is about twice higher than that of Co ( $T_{WC}=2870^{\circ}\text{C}$  and  $T_{Co}=1495^{\circ}\text{C}$ ) [9, 16]. During the laser ablation, Co undergoes melting and vaporization first, while WC only experiences melting. However, the ablation dynamics can be more complex when laser-matter reaction occurs in air atmosphere. Under these conditions, carbon (C) from WC grains can react with oxygen ( $\text{O}_2$ ) existing in the atmosphere, yielding as resulting formation of CO and  $\text{CO}_2$ . The steam pressure caused by the formation or vaporization of CO/ $\text{CO}_2$  promotes the ejection of liquid material in a recoil action, leading then to the production of pores in the laser-matter reaction area [7, 9-10, 17-19]. As a consequence, the expelled liquid is put aside from the reaction center to its edge, producing a crown-like structure on the edge of the dimple.

Nowadays, the implementation of laser beam machining is becoming popular as surface modification treatment for cemented carbides, whereas the action is usually referred to as laser surface texturing (LST). Some innovative patterns, such as micro-grooves, micro-pits and dimples, have been produced on certain materials. It has been reported that these structures may enhance tribological properties of the contact surfaces as they can serve as micro-traps for wear debris in either lubricated or dry sliding [12, 13]. However, to the best knowledge of the authors, literature reports on LST of cemented carbides have mainly focused on presenting tribological response attained by the application of certain innovative surface patterns [8, 17-18, 20-21]. On the other hand, information about the laser ablation mechanism of cemented carbides is rather scarce. This includes investigations on the influence of laser intrinsic parameters, such as pulse duration, energy level etc. as well as laser machining parameters on the geometrical precision of the resulting surface structures.

Following the ideas mentioned above, the main objective of this study is to carry out an investigation addressing the influence of pulse number at three different pulse energy levels on the ablation of cemented carbides. The study also involves microstructural effects by considering two cemented carbide grades with similar chemical compositions but different grain size on laser ablation. Geometrical properties of the produced dimples, i.e. diameter, depth and height of the eventually induced crown-like structure, are obtained by means of Laser Scanning Microscopy (LSM) and White Light Interferometry (WLI). Surface integrity assessment is accomplished by combined Field Emission Scanning Electron Microscopy-

Focused Ion Beam (FESEM-FIB) which allows the examination of the transversal section of the dimple.

## 2. Experimental aspects

### 2.1. Investigated materials

Two cemented carbides, referred to as 10CoC and 11CoM, were selected as investigated materials. They are plain grades composed with tungsten carbides (WC) as hard phase and cobalt (Co) as binder. Figure 1 shows the microstructures of the investigated materials. There, the gray phase indicates WC and the black one indicates Co. It can be observed that 11CoM has finer grains than 10CoC. Microstructural properties of these two grades are listed in Table 1. The cobalt contents are 10 %wt and 11 %wt for 10CoC and, respectively, 11CoM. Mean grain size of 10CoC is about  $2.33\ \mu\text{m}$ , approximately twice as big as the one of 11CoM, i.e.  $1.12\ \mu\text{m}$ .

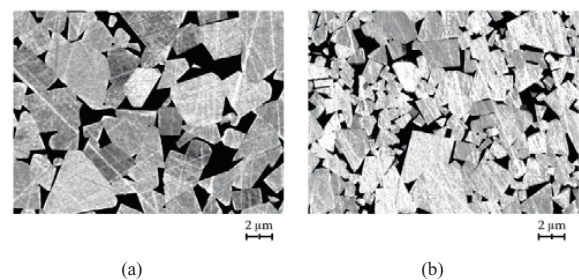


Fig. 1. Polished surfaces of the investigated materials, images taken by SEM: (a) 10CoC and (b) 11CoM.

Table 1. Microstructural and basic mechanical properties of the cemented carbide grades investigated.

Specimen	Binder	$V_{\text{binder}}$ (%wt)	$d_{\text{WC}}$ ( $\mu\text{m}$ )	HV30 (GPa)	Fracture toughness $K_{\text{Ic}}$ ( $\text{MPa}\sqrt{\text{m}}$ )
10CoC	Co	10	$2.33 \pm 1.38$	$11.4 \pm 0.2$	$15.8 \pm 0.3$
11CoM	Co	11	$1.12 \pm 0.71$	$12.8 \pm 0.2$	$13.9 \pm 0.3$

### 2.2. Experimental design

A solid-state Nd:YLF, Q-switched laser set-up (Explorer® One™ Spectra Physics) is employed to produce dimples on the target surfaces. The set-up is capable to emit laser beams having the wavelength of 349 nm, the pulse duration of 5 nanoseconds (FWHM, namely Full Width at Half Maximum), and the nominal pulse repetition frequency of 1000 Hz (Table 2). Figure 2 illustrates the configuration of the laser machining platform. A 2-axis laser beam deflection unit (Raylase) is applied to control the movement of the focus point on the XY-plan. Two additional mirrors are set up to adjust the trajectory of the laser beams. The sample is fixed on the sample holder which is equipped with Vernier calipers along the x-, y- and z-axis. The focal length, i.e. the distance between the lens and the target surface, is set to 132 mm.

Table 2 Laser parameters used in this study.

Laser type	Laser source	Pulse duration (ns)	Wave length (nm)	Frequency (Hz)
ns-laser	Nd:YLF	5	349	1000

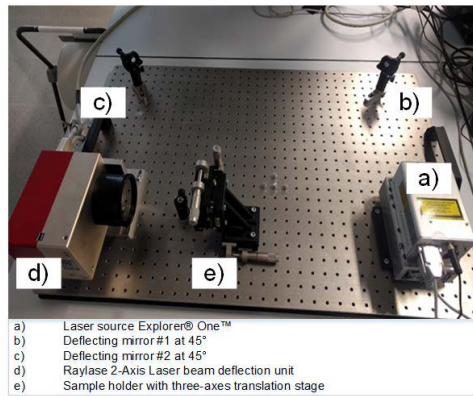


Fig. 2. Configuration of the precise laser machining platform.

In the experiments, three different levels of laser pulse energy are applied to produce the dimples, i.e. 130  $\mu\text{J}$ , 65  $\mu\text{J}$  and 13  $\mu\text{J}$ . For each level, the pulse number was chosen within the range from 10 to 120, with 10 pulse intervals. Each experimental combination was repeated three times (Figure 3(a)). Three geometrical parameters for describing shape and dimension of the dimples were characterized: diameters  $d_1$  and  $d_2$  along the x- and y- axis, and depth  $h$ . A crown-like structure was discerned in several cases. There, height  $a_1$  and  $a_2$  at the marked positions (Figure 3(b)) were measured. Based on the measurements, the average value of the diameters and heights, i.e.  $d$  and  $a$ , were then obtained.

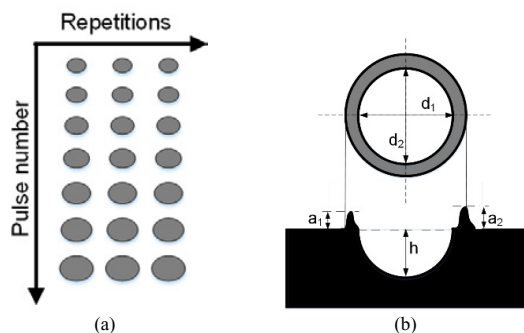


Fig. 3. (a) Arrangement of dimples produced on the surface of cemented carbides, (b) characterization of geometrical properties.

### 3. Results and discussion

#### 3.1. Geometrical property characterization

Figure 4 illustrates dimple diameter as a function of the pulse number at three different laser energy levels for both cemented carbide grades. Independent of microstructure, the dimple diameter increases along with the applied laser energy. Furthermore, the diameter variation is more pronounced at a low energy level. For example, at the pulse number of 60, when the applied laser energy increases from 13  $\mu\text{J}$  to 65  $\mu\text{J}$ , the diameter increases about 15  $\mu\text{m}$  and 25  $\mu\text{m}$  for 10CoC and 11CoM, respectively. However, the rise from 65  $\mu\text{J}$  to 130  $\mu\text{J}$  is less obvious, i.e. only about 8  $\mu\text{m}$  for both grades. The

observation is caused by the fact that the ablation threshold of the cemented carbides is roughly situated between 13  $\mu\text{J}$  and 65  $\mu\text{J}$  which corresponds to the minimum necessary laser energy to melt cobalt [22, 23]. When the applied energy is less than the threshold, few ablation exhibits; in contrary, large ablation occurs brutally but not continuously in terms of the diameter expansion since the laser beam has a Gaussian profile and the width of its energy band is stable.

At the given laser energy level, grade 11CoM exhibits a larger diameter than 10CoC, except at the lowest energy level. However, the differences are quite small. When the pulse number increases, the diameter does not show much difference compared to the initial conditions, since the diameter of the laser beam does not change in the experiments. In Figure 4, some points are not shown, because the slightly processed material surface is difficult to characterize using optical microscopies at low level energy, or the structures would be destroyed at high level energy.

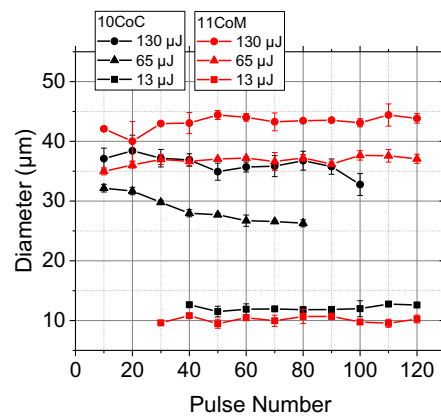


Fig. 4. Diameter evolution as a function of the pulse number.

Figure 5 illustrates the dimple depth as a function of the pulse number at three different laser energy levels for both investigated grades. It is obvious that higher applied energy produces deeper dimples, and the dimple depth is proportional to the pulse number at the energy levels of 65  $\mu\text{J}$  and 130  $\mu\text{J}$ . However, such an increase does not take place at the energy level of 13  $\mu\text{J}$  which is not sufficient to ablate both Co and WC. When the comparison is made at one grade between different energy levels i.e. 65  $\mu\text{J}$  and 130  $\mu\text{J}$ , the depth of the dimples produced by 130  $\mu\text{J}$  is approximately twice as much as the one produced by 65  $\mu\text{J}$ . The depth evolution of 10CoC at the energy level of 130  $\mu\text{J}$  is shown with a dashed line, since the depth is beyond the capacity of the measurement equipment.

When comparing these two grades within identical pulse number, the laser beam with identical energy level produces dimples much deeper at 10CoC than at 11CoM. The observation is in agreement with the one reported in [23] where higher dimple depth was attained in a cemented carbide with grain size of 1.5  $\mu\text{m}$ , as compared to another one with the grain size of 0.5  $\mu\text{m}$ . Taking into account the obtained dimple diameter presented in Figure 4, it can be concluded that coarser microstructures lead to larger dimple depths but smaller diameters. It may be rationalized by considering both material and laser aspects.

Although the two components of the cemented carbides have comparable thermal conductivity, i.e. WC: 60–80 W/m K, Co: 70–75 W/m K, the ablation threshold of WC is higher than that of Co due to their different melting points, i.e. WC: 2870 °C, Co: 1495 °C. [22, 23]. Accordingly, large WC grains form a barrier which obstructs the energy expansion due to its high thermal conductivity. When the sample surface is impinged by the laser, temperature increases rapidly, reaching and surpassing the melting temperature of the metallic Co binder [17]. As a result, the Co binder will be evaporated faster from the surface than the WC grain. Thus, the availability of the Co binder at the center of the laser spot (where the energy is concentrated), is depleted quickly, and the WC particles are exposed. Since coarse WC grains serve as a barrier and lead the concentration of the laser energy, it is much easier for the laser beam to conduct more ablation of the Co binder, as the microstructure gets coarser. Moreover, at higher energies, the reached temperature can be higher than the one required for melting WC particles; thus, partial or complete melting of the WC grains can also occur. As this is expected to be easier as carbides gets finer, the entire ablation is less obvious at 11CoM.

Regarding the laser beam, its Gaussian profile leads to higher energy concentration and more ablation in vertical direction. Therefore, the depth is more pronounced in the case of 10CoC because of the coarse carbides. It is also observed that the depth increases proportionally with the grain size. At the energy level of 65 μJ and pulse number of 60, for example, the dimple depth of 10CoC (grain size 2.33 μm) is 35 μm, approximately twice as much as the one of 11CoM (grain size 1.12 μm).

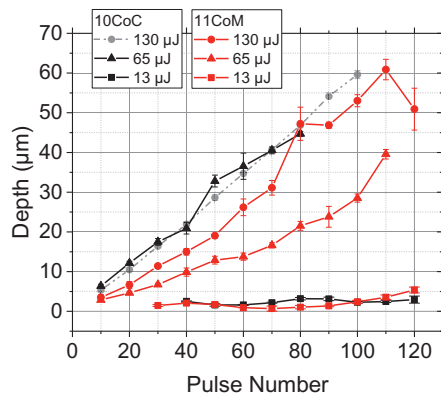


Fig. 5. Depth evolution as a function of the pulse number.

As the material ablation increases, so does the height of the accumulated re-deposition which forms the crown-like structure around the edge of the dimple [24]. Figure 6 shows the re-deposition height as a function of the pulse number at different energy levels. When the applied energy increases for each grade, the height of crown-like structure increases. At a low energy level, the re-deposition is not obvious and can be disregarded. However, at a high laser power, the height of the crown-like structures seems to be approximately proportional to the pulse number. However, such trend is not continuous, and the increase of the height slows down as the energy increases, since more ablation occurs and the re-deposition may

also be destroyed. It can also be observed that the height obtained at 10CoC is slightly greater than that at 11CoM, but the differences are not evident.

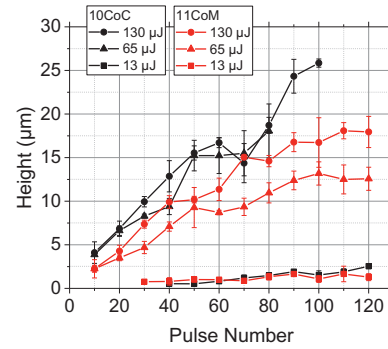


Fig. 6. Height evolution as a function of the pulse number.

### 3.2. Surface morphology inspection

Figure 7 shows the surface morphological inspection of the two cemented carbide grades after the application of 70 pulses at three different pulse energy levels. At the low energy level of 13 μJ, only poor ablation is induced. Given the Gaussian shape of the laser beam, it can be expected that the energy distribution of the beam widens as the laser energy increases. Thus, the laser affected zone (HAZ) is expected to become larger when the applied pulse energy increases. At each energy level, the difference of HAZ induced at 11CoM and at 10CoC are not evident. The material response to laser ablation in terms of grain size results then in little geometrical difference such as diameter variation.

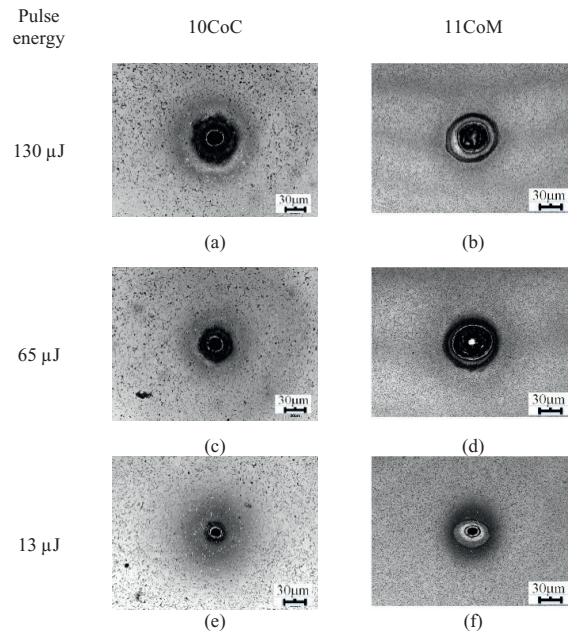


Fig. 7. Surface morphology of the produced dimples on 10CoC and 11CoM grades, with 70 pulses and different pulse energies.

Figure 8 shows morphology and cross-sectional inspection carried out by SEM-FIB. It is clear that both dimples are

covered by a grey circle in Fig 8 (a) and (c), which are the heat affected zones (HAZ). HAZ expands from the centre to the edge of the dimple and leaves a grey crown surrounding it. This represents a slight re-deposition layer of the melted binder as a consequence of the laser ablation. The distribution of the re-deposition layer meets the Gaussian profile of the laser beam and can be observed in the cross-sectional inspection in Figure 8(b) and (d) for both grades. The interior of the dimples produced on the two cemented carbides exhibits different morphology. The dimple at 10CoC is filled with some flocs, whereas the one at 11CoM shows a complete bowl profile (Figure 8(a) and (c)). The flocs filled in the dimple produced at 10CoC are the stack of the recast material, and eventually the stack of the clasped crown-like structures. The observation is not pronounced in the case of 10CoM, except at some positions where the crown-like structure slightly clasps. This observation proves that laser ablation is more pronounced at the finer grade. Certain defects, such as pores and flaws, have also been induced on the inner surface by the laser ablation, which are inherent to the melting, vaporization and solidification processes (Figure 8(c)).

Cross-sectional inspection of both grades presents more details of the laser induction. It is found that the re-deposition layer is about several micrometers thick and more pronounced in the case of 10CoC (Figure 8(b) and (d)). Pores and micro-cracks are concentrated on the surface and do not penetrate into the matrix. It can be assumed that micro-cracks are originated from the residual stresses, which are induced by thermal expansion and contraction. The recast layer is rather porous and brittle. The study reported by Tan et al. [25] suggests that the porosity is due to a reduction of material density as a result of the high laser energy and chemical interactions.

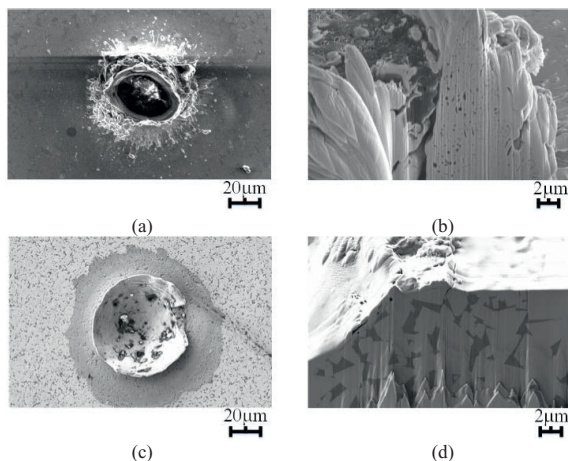


Fig. 8. Dimple produced by 70 laser pulses with the energy 130  $\mu$ J: SEM characterization of (a) 10CoC and (c) 11CoM, FIB cross-sectional analysis of (b) 10CoC and (d) 11CoM.

#### 4. Conclusions

In this study, short pulse laser beams have been applied with three energy levels at two WC-Co cemented carbide grades with similar chemical composition but different grain size. Geometrical properties of the laser induced dimples have been

studied as well as its surface integrity. The following conclusions can be drawn:

- Laser ablation is very poor at low energy level, but becomes obvious when the applied energy passes certain level. Afterwards, the laser ablation is approximately proportional to the energy increase. However, the exact ablation is not clear, it would be therefore interesting to carry out research on the determination of the exact ablation threshold for different cemented carbide grades.
- Carbide grain size plays a very important role in the laser ablation phenomenon. The coarser the microstructure is; the deeper ablation is evidenced under identical machining conditions. However, the observation is not evident in terms of the dimple diameter. In the future, it would be important to study the influence of the intrinsic parameters, such as binder content and additives.
- The laser affected zone was covered by a very thin recast layer and the laser induced defects (such as pores and micro-cracks) were only found at the subsurface. The induced crown-like structures are quite brittle and porous and they become more pronounced when the applied laser pulse increases.

#### Acknowledgements

The work leading to this publication was supported by the German Academic Exchange Service (DAAD) with funds from the German Federal Ministry of Education and Research (BMBF) and the People Program (Marie Curie Actions) of the European Union's Seventh Framework Program (FP7/2007-2013) under REA grant agreement n° 605728 (P.R.I.M.E. – Postdoctoral Researchers International Mobility Experience). The authors are grateful for the material supplying by Sandvik Hard Materials R&D Division (Coventry, UK). Finally, this contribution has also been partly funded by the Spanish Ministry of Economy and Competitiveness through Grant MAT2015-70780-C4-3P (MINECO/FEDER).

#### References

- [1] Bhaumik SK, Upadhyaya GS, Vaidya ML. A transmission electron microscopy study of WC-10Co cemented carbides with modified hard and binder phases. *Materials Characterization* 1992;28:241–9. doi:10.1016/1044-5803(92)90085-V.
- [2] Fang ZZ, Koopman MC, Wang H. Cemented Tungsten Carbide Hardmetal- An Introduction. *Comprehensive Hard Materials*, vol. 1, 2014, p. 123–37. doi:10.1016/B978-0-08-096527-7.00004-0.
- [3] Tsuda K. History of development of cemented carbides and cermet. *SEI Technical Review* 2016:16–20.
- [4] Upadhyaya G. Materials science of cemented carbides — an overview. *Materials & Design* 2001;22:483–9. doi:10.1016/S0261-3069(01)00007-3.
- [5] Schubert WD, Lassner E, Bohlke W. Cemented carbides-a success story. *Tungsten, Int, Tungsten Industry Association (ITIA)*(June 2010) 2010:12.
- [6] Tarragó JM, Dorvlo S, Esteve J, Llanes L. Influence of the microstructure on the thermal shock behavior of cemented carbides. *Ceramics International* 2016;42:12701–8. doi:10.1016/j.ceramint.2016.05.024.
- [7] Karpuschewski B, Wolf E, Krause M. Laser Machining of Cobalt Cemented Tungsten Carbides BT - Towards Synthesis of Micro-/Nano-systems: The 11th International Conference on Precision Engineering (ICPE) August 16–18, 2006, Tokyo, Japan. In: Kimura F, Horio K, editors., London: Springer London; 2007, p. 243–8. doi:10.1007/1-84628-559-3\_41.

- [8] Dumitru G, Romand V, Weber HP, Gerbig Y, Haefke H, Bruneau S, et al. Femtosecond laser ablation of cemented carbides: Properties and tribological applications. *Applied Physics A: Materials Science and Processing* 2004;79:629–32. doi:10.1007/s00339-004-2675-1.
- [9] Neves D, Diniz AE, Lima MSF. Microstructural analyses and wear behavior of the cemented carbide tools after laser surface treatment and PVD coating. *Applied Surface Science* 2013;282:680–8. doi:10.1016/j.apsusc.2013.06.033.
- [10] Chichkov BN, Momma C, Nolte S, von Alvensleben F, Tünnermann A. Femtosecond, picosecond and nanosecond laser ablation of solids. *Applied Physics A: Materials Science & Processing* 1996;63:109–15. doi:10.1007/s003390050359.
- [11] Stafe M, Marcu A, Puscas NN. Pulsed Laser Ablation of Solids. vol. 53. 2014. doi:10.1007/978-3-642-40978-3.
- [12] Dieter W. Bäuerle. *Laser Processing and Chemistry*. Springer, vol. 208, 2011, p. 279–313. doi:10.1524/zpch.1999.208.Part\_1\_2.291a.
- [13] Kumar A, Gupta MC. Laser machining of micro-notches for fatigue life. *Optics and Lasers in Engineering* 2010;48:690–7. doi:10.1016/j.optlaseng.2010.01.008.
- [14] von Allmen M, Blatter A. *Laser-Beam Interactions with Materials*. 1995. doi:10.1007/978-3-642-57813-7.
- [15] Ion JC. *Laser Processing of Engineering Materials: Principles, Procedure and Industrial Application*. Laser Processing of Engineering Materials, 2005, p. 576. doi:0750660791.
- [16] Li T, Lou Q, Dong J, Wei Y, Liu J. Selective removal of cobalt binder in surface ablation of tungsten carbide hardmetal with pulsed UV laser. *Surface and Coatings Technology* 2001;145:16–23. doi:10.1016/S0257-8972(01)01288-9.
- [17] Dumitru G, Romano V, Weber HP, Haefke H, Gerbig Y, Pflüger E. Laser microstructuring of steel surfaces for tribological applications. *Applied Physics A: Materials Science and Processing* 2000;70:485–7. doi:10.1007/s003390051073.
- [18] Karatas C, Yilbas BS, Aleem A, Ahsan M. Laser treatment of cemented carbide cutting tool. *Journal of Materials Processing Technology* 2007;183:234–40. doi:10.1016/j.jmatprotec.2006.10.012.
- [19] Sokolowski-Tinten K, Bialkowski J, Cavalleri A, von der Linde D, Oparin A, Meyer-ter-Vehn J, et al. Transient States of Matter during Short Pulse Laser Ablation. *Physical Review Letters* 1998;81:224–7. doi:10.1103/PhysRevLett.81.224.
- [20] Fang S, Herrmann T, Rosenkranz A, Gachot C, Marro F.G., Mücklich F., Llanes L, Bähre D, 2016. Tribological performance of laser patterned cemented tungsten carbide parts. *Procedia CIRP* 42, 439–443. doi:10.1016/j.procir.2016.02.228
- [21] Fang S, Llanes L, Bähre D. Wear Characterization of Cemented Carbides (WC-CoNi) Processed by Laser Surface Texturing under Abrasive Machining Conditions. *Lubricants* 2017;5:20. doi:10.3390/lubricants5030020.
- [22] Li T, Lou Q, Dong J, Wei Y, Liu J. Phase transformation during surface ablation of cobalt-cemented tungsten carbide with pulsed UV laser. *Applied Physics A* 2001;73:391–7. doi:10.1007/s003390100745.
- [23] Dumitru G, Romano V, Weber HP, Sentis M, Marine W. Femtosecond ablation of ultrahard materials. *Applied Physics A: Materials Science and Processing* 2002;74:729–39. doi:10.1007/s003390101183.
- [24] Leitz KH, Redlingshöfer B, Reg Y, Otto A, Schmidt M. Metal ablation with short and ultrashort laser pulses. *Physics Procedia*, vol. 12, 2011, p. 230–8. doi:10.1016/j.phpro.2011.03.128.
- [25] Tan JL, Butler DL, Sim LM, Jarfors AEW. Effects of laser ablation on cemented tungsten carbide surface quality. *Appl Phys A* 2010;101:265–9. doi:10.1007/s00339-010-5815-9.